

## Self-consistent electronic spectrum of trigonal Te. Charge and momentum density, and Compton profile

P. Krusius\* and T. Stubb

*Electron Physics Laboratory, Helsinki University of Technology, and Semiconductor Laboratory, Technical Research Center of Finland SF-02150 Espoo 15, Finland*

H. Isomäki

*Department of General Science, Helsinki University of Technology, SF-02150 Espoo 15, Finland*

J. von Boehm<sup>†</sup>

*NORDITA, DK-2100 Copenhagen Ø, Denmark*

(Received 14 December 1980)

The electronic ground state of crystalline trigonal tellurium has been determined according to a self-consistent local-density-dependent approach with the Slater  $X\alpha$  exchange correlation, and with orthogonalized-plane-wave and linear-combination-of-atomic-orbitals representations for valence and core states. Results are given for the valence electron charge and momentum density, the Compton profile, and the autocorrelation function of the one-electron density matrix. These quantities are discussed with respect to trigonal selenium, since no experimental data are available for these quantities for Te. A discussion of the chemical bonding in trigonal Te is given.

### I. INTRODUCTION

Experimentally the ground-state charge and momentum densities of electrons in a solid are accessible via elastic and inelastic photon scattering. The former gives the radial distribution function and the x-ray form factors, and the latter results in the Compton profile<sup>1</sup> or the Fourier-transformed Compton profile, which is equivalent to a spatial average of the off-diagonal elements of the one-electron density matrix. Despite these facts, models for electrons in solids are not often carried beyond energy spectra to include charge and momentum densities. For the  $sp^n$ -bonded semiconductors only for trigonal selenium,<sup>2-4</sup> and partly for tetrahedral diamond<sup>5</sup> and silicon,<sup>6</sup> such a program has been completed. Results obtained have included information on the chemical bond both in position and momentum space for the crystalline<sup>3,4</sup> as well as the polycrystalline and amorphous phases.<sup>4,7,8</sup>

This study is an extension of the selenium work to the closely related tellurium. Both crystallize in the trigonal phase (*t*-Te, *t*-Se) with helical chains packed into a hexagonal lattice (space group  $D_3^2$ ). The main objective is to investigate differences in bonding between the molecular-type *t*-Se and the more metallic *t*-Te. The charge density, the momentum density, the Compton profile, and the autocorrelation function of *t*-Te are hence discussed with respect to previous results for *t*-Se.<sup>3,4</sup> Energy spectra and related properties of the present model for *t*-Te are given elsewhere.<sup>9</sup> Some preliminary results for *t*-Te have been published earlier,<sup>10</sup> and discussed with other

phases of Se and Te together with a review of the symmetry properties of the present quantities elsewhere.<sup>8</sup> This paper, however, together with another<sup>9</sup> contains a full description of all these results for the trigonal phase of Te.

Some computational changes have been made for the parameters of *t*-Te in comparison to *t*-Se.<sup>3,4</sup> The number symmetrized OPW's at each of the six sampling points is 235. The momentum mesh in the irreducible wedge of the first Brillouin zone includes  $8 \times 10 = 80$  points. 145 or 159 OPW's and 339 or 351 plane waves are used in the projection procedure at each general  $\bar{k}$  point for  $\alpha = 1$  or  $\frac{2}{3}$ , respectively. The momentum space cutoff radius is 3.3 times the Fermi momentum of an isotropic free-electron gas with equal density. The overall convergence properties at the 336 960 momentum space points ( $\alpha = \frac{2}{3}$ ) are comparable to those for *t*-Se.<sup>3,11</sup> In Secs. II–V the charge density, the momentum density, the Compton profile, and the autocorrelation function of the one-electron density matrix are presented and discussed. The paper ends with general remarks on bonding for *t*-Te and *t*-Se.

### II. CHARGE DENSITY

The valence-electron charge density (VCD)  $\rho_v(\bar{r})$  for *t*-Te associated with the  $\alpha = \frac{2}{3}$  model is displayed in the usual contour plane in Fig. 1 and as a one-dimensional graph in Fig. 2. A plot for  $\alpha = 1$  has been published elsewhere.<sup>10</sup> Additional information

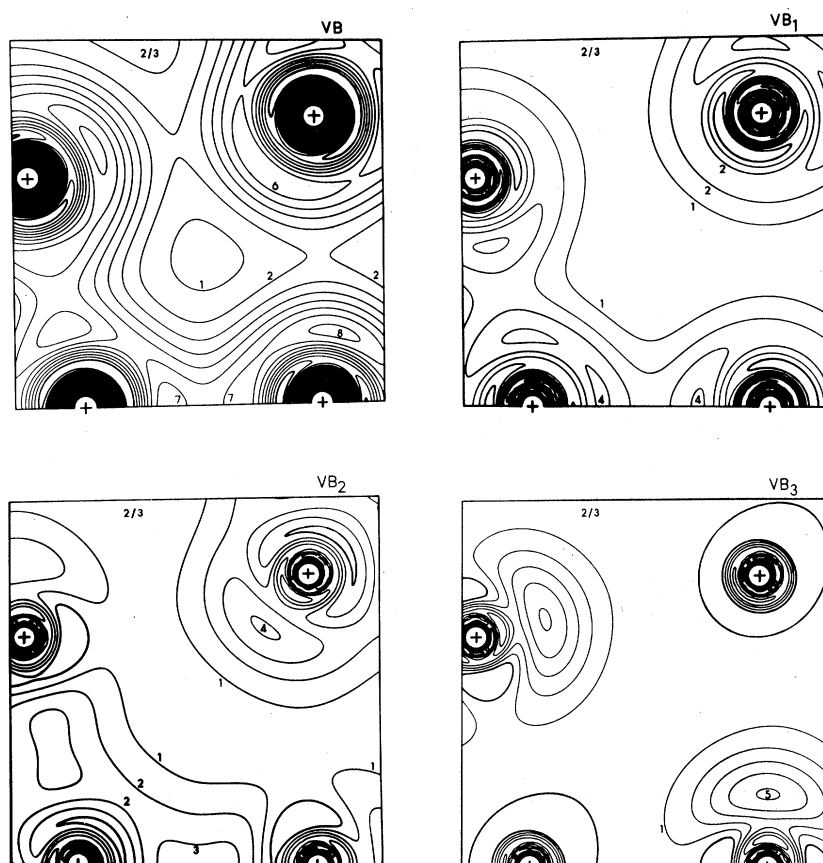


FIG. 1. Valence-electron charge density  $\rho_v(\vec{r})$  of *t*-Te for  $\alpha = \frac{2}{3}$  as a contour plot. VB denotes the total valence charge and  $VB_1$ ,  $VB_2$ , and  $VB_3$  the triplet contributions. Each contour plane contains four atom sites all marked with crosses. The upper left, lower left, and lower right sites are adjacent atoms in the same helical chain. The diagonal from the lower left to the upper right site is along the *a* axis and its length is equal to the lattice constant *a*. Because of the strong orthogonality oscillations with the core, contour separations at the sites are so small that these regions appear black. The contour separation is always 0.01 a.u., i.e.,  $e/a_0^3$  where *e* denotes the electron charge and  $a_0$  the Bohr radius.

on the charge densities and other one-dimensional graphs are also given elsewhere.<sup>12</sup> Qualitatively the VDC remains unaffected, if  $\alpha$  is increased from  $\frac{2}{3}$  to 1, but quantitatively the structures in the VCD tend to localize and sharpen.

VCD contour plots for *t*-Te have been obtained earlier from the conventional empirical pseudopotential method<sup>13,14</sup> (EPM) and the self-consistent EPM<sup>15</sup> (SCEPM) approach. All pseudopotential VCD's are very similar. The SCEPM VCD is for all valence-band triplets least localized, witnessing the importance of self-consistency in determining wave functions. The SCEPM model, having two adjustable parameters, bears most close resemblance to the SCOPW results without any adjustable parameters.

The SCOPW VCD's display however better resolved details in all charge densities. Similar findings have been made also in connection with other first-principles methods, such as in the *ab initio* Hartree-Fock-Slater study of the  $Si_2$  dimer.<sup>16</sup>

A comparison of the *t*-Te triplet VCD's  $VB_1$ ,  $VB_2$ , and  $VB_3$  (Fig. 1) and total VCD with those of *t*-Se (Refs. 3 and 8) reveals important differences. Because of differences in the lattice constants, the average charge density is about 20% lower in *t*-Te than in *t*-Se. In addition the *t*-Te  $VB_1$  and  $VB_2$  VCD's are more delocalized and show a more cubic character compared to *t*-Se.<sup>17</sup> This indicates the presence of significant changes in the intrachain versus interchain bonding.

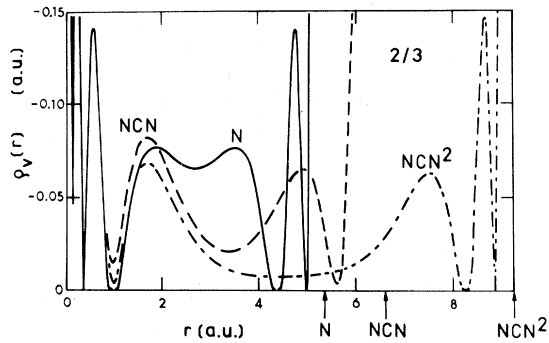


FIG. 2. Valence-electron charge density  $\rho_v(\vec{r})$  of  $t$ -Te for  $\alpha = \frac{2}{3}$  as a function of  $r$  along characteristic directions. The plots start for all three directions from the same reference atom in the left corner. The directions are: nearest-neighbor direction within the chain (N), next-nearest-neighbor direction to nearest chain next atom (NCN), and to nearest chain next-nearest atom (NCN<sup>2</sup>). Atom sites are denoted with arrows and labeled according to the directions. Each curve ends along each ray, when it for the first time crosses the boundaries of the plot. Orthogonality oscillations are thus shown correctly only for the reference atom.  $\rho_v$  and  $r$  are given in a.u.

### III. MOMENTUM DENSITY

The valence-state momentum density (VMD)  $N_v(\vec{p})$  for  $t$ -Te with  $\alpha = \frac{2}{3}$  is shown in Fig. 3. The result for  $\alpha = 1$  and the atomic momentum density (AMD) for the configuration  $5s^25p^4$ , based on closed-shell double  $\zeta$  restricted Hartree-Fock (RHF) results, have been presented elsewhere.<sup>8,10</sup> The characteristic extent of the VMD may be obtained from the isotropic free-electron (FE) approximation. For an equal density this results in a Fermi radius  $p_F = 0.918$  a.u. One finds qualitatively unchanged results for  $\alpha$  in the range  $(\frac{2}{3}, 1)$ . Since the VMD is in complementary space to the VCD, an increasing  $\alpha$  from  $\frac{2}{3}$  to 1 should delocalize the VMD. This trend is confirmed for  $t$ -Te.  $N_v(0)$  for  $\alpha = \frac{2}{3}$  is 5.3% higher than for  $\alpha = 1$ . For unchanged orbitals this should be interpreted as an increase of the  $s$ -like admixture into the ground state by an equal amount from 1 to  $\frac{2}{3}$ . But, since the localization of orbitals has been shown to change slightly, most of the change 5.3% is to be attributed to the latter effect.

The effect of bond formation on the momentum density of  $sp^n$ -bonded systems in crystalline directions in general and for  $t$ -Se in particular has been discussed elsewhere.<sup>3</sup> Compared to  $t$ -Se (Ref. 3) the  $t$ -Te VMD is for both directions shown to be much more free electronlike, an expression of the more

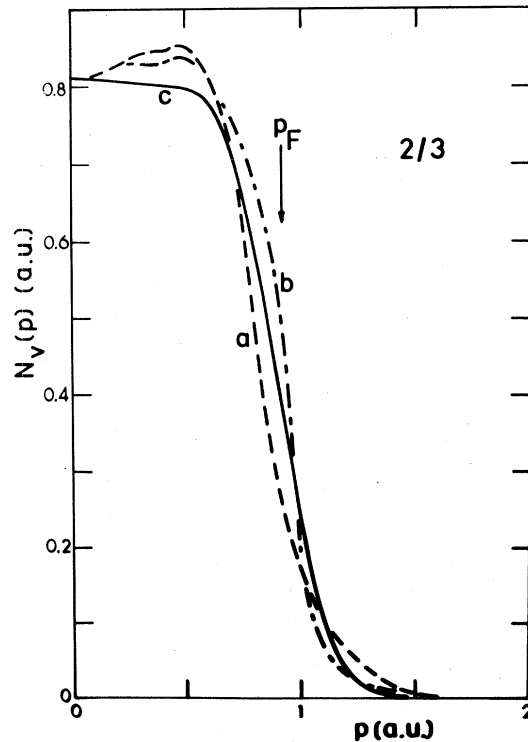


FIG. 3. Valence-electron momentum density  $N_v(\vec{p})$  of  $t$ -Te for  $\alpha = \frac{2}{3}$  along characteristic directions from the origin  $\vec{p} = 0$  as a function of  $\vec{p}$ . The directions shown are the  $c$  axis (c),  $a$  axis (a) and the reciprocal-lattice vector perpendicular to the  $c$  axis (b). The angle between directions  $a$  and  $b$  is  $15^\circ$ .  $N_v(\vec{p})$  is normalized such that the integral of  $2\Omega_0/(2\pi)^3 N_v(\vec{p})$  over all momentum space gives the number of valence electrons in the unit cell, i.e., for  $t$ -Te 18.  $\Omega_0$  denotes the unit cell volume and  $p_F$  the Fermi momentum of an isotropic free-electron gas with equal density. Atomic units are used for  $N_v$  and  $p$ .

metallic character of Te. Second, evidently the anisotropy of the VMD for  $t$ -Te is smaller than for  $t$ -Se, although the structure otherwise appears to be qualitatively similar.

### IV. COMPTON PROFILE

The valence Compton profiles (VCP)  $J_v(q)$  associated with the  $\alpha = \frac{2}{3}$  and 1 SCOPW ground-state models are given in Table I for  $t$ -Te. The RHF core profile has been included for completeness.<sup>8</sup> Figure 4 displays the anisotropy of the VCP for both values of  $\alpha$ . The effect of bond formation on the VCP with respect to the atomic counterpart<sup>8</sup> (ACP) from the configuration  $5s^25p^4$  are seen to occur in a similar fashion as in the VMD, except that, because of the

TABLE I. Valence-state Compton profile  $J_v(q)$  from the SCOPW ground-state model and part of the RHF core-state Compton profile  $J_c(q)$  (shells  $1s-4d$ ) (Ref. 8) of  $t$ -Te as a function of momentum  $q$ .  $J_v(q)$  is given for  $\vec{k}$  along the  $c$  axis ( $c$ ) or along the  $a$  axis ( $a$ ). The columns for  $J_v(q)$  are labeled with the directions  $c$  and  $a$  and the exchange-correlation constant  $\alpha = \frac{2}{3}$  or 1. All entries are in a.u., i.e., for  $q(1/a_0)$ , where  $a_0$  denotes the Bohr radius. The sum ( $J_c + J_v$ ) has been normalized to the number of electrons in the unit cell, i.e., 156.

$q$	$J_v(q)$		$J_c(q)$		$J_c(q)$
	$\frac{2}{3}, c$	$\frac{2}{3}, a$	1, $c$	1, $a$	
0	13.084	12.890	13.005	12.586	15.273
0.2	12.671	12.452	12.586	12.143	15.236
0.4	10.879	10.672	10.698	10.491	15.121
0.6	7.786	7.847	7.690	7.785	14.923
0.8	3.990	3.941	4.113	4.137	14.632
1.0	1.149	1.251	1.309	1.539	14.235
1.2	0.493	0.601	0.573	0.743	13.721
1.4	0.349	0.406	0.386	0.465	13.096
1.6	0.324	0.312	0.342	0.333	12.526
1.8	0.290	0.258	0.298	0.261	11.586
2.0	0.216	0.269	0.222	0.252	10.761
2.2	0.161	0.223	0.174	0.216	9.932
2.4	0.131	0.150	0.143	0.154	9.126

integration involved, the parallel and perpendicular directions are interchanged. Thus, for small momenta  $J_v(q)$  along the  $c$  axis should lie higher than along the  $a$  axis, and for intermediate momenta vice versa, of course.

Although the CP of  $t$ -Te has not yet been measured, there are data for  $t$ -Se both from 60 keV Am

$\gamma$ -ray<sup>18,4</sup> and from 412 keV Au  $\gamma$ -ray<sup>19</sup> experiments. Discussions of the Se results published elsewhere<sup>8</sup> have shown, that the present approach gives an excellent description of the CP and the FCP both for trigonal crystalline and polycrystalline Se. This fact should then give some faith in the predictions presented for  $t$ -Te.

Compared to  $t$ -Se (Ref. 3) the anisotropy of the VCP of  $t$ -Te is seen to show the same qualitative behavior. The overall magnitude is, however, by a factor of about 2 smaller in  $t$ -Te. This effect was already seen in the VMD and is simply an expression of the more metallic character of  $t$ -Te. The similarity of the anisotropy of the VCP of  $t$ -Te and  $t$ -Se gives reason to believe that the nature of this anisotropy may be explained by pure structural and occupational effects.<sup>20</sup>

## V. AUTOCORRELATION FUNCTION

The one-dimensional Fourier transform of the CP is in the impulse approximation equal to the autocorrelation function (AF) of the one-electron density matrix  $\Gamma_1(\vec{r}, \vec{r}')$ , i.e.,

$$B(\vec{r}) = \int d^3r' \Gamma_1(\vec{r}, \vec{r} + \vec{r}). \quad (1)$$

A simple physical interpretation of this function, ex-

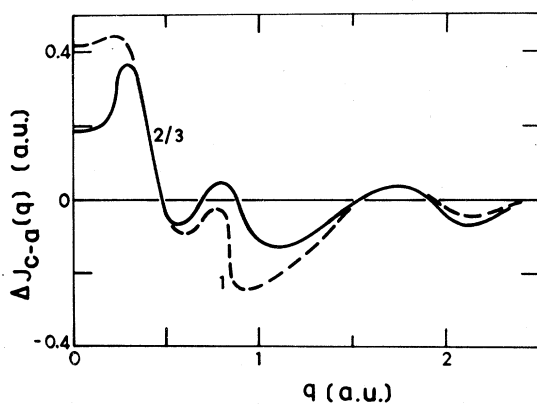


FIG. 4 Anisotropy of valence-electron Compton profile  $\Delta J_{c-a}(q)$  for  $t$ -Te with  $\alpha = \frac{2}{3}$  and 1 as a function of  $q$ . Directions, labels, and normalization are explained in caption of Table I.

cept for the lattice translation zeros, does not yet exist, but considerable progress has been obtained by studying its properties for several model systems of solids.<sup>20,21-23</sup> The simple limiting cases given by the single isolated atom and the free-electron gas may also be used.<sup>8</sup>

The valence autocorrelation function (VAF)  $B_v(\vec{r})$  for  $t$ -Te for both values of  $\alpha$  is given in Figs. 5 and 6.<sup>12</sup> The core-state contributions of  $t$ -Te to the autocorrelation function are significant only for  $t \leq 3$  a.u. The  $B_v(\vec{r})$  results for  $t$ -Te display the same general properties, which have been discussed for real semiconductors<sup>4</sup> like Se and for one-dimensional ordered and disordered model systems<sup>21</sup> elsewhere. A measure of the accuracy of the present results may be obtained from the position of the lattice zeros. The relative errors of the first lattice zeros at  $c$  and  $a$  are for both  $\alpha$ 's 0.32 and 0.10%, respectively, which is quite surprising considering the numerous calculational steps performed after the one-electron states

were solved for. The effect of  $\alpha$  on  $B_v(\vec{r})$  is quite predictable once the influence on  $J_v(q)$  is known. In fact, the ground-state model with  $\alpha = \frac{2}{3}$  shows stronger correlations, as measured by the amplitudes of the VAF, than the result with  $\alpha = 1$ . Since again no experimental data is available for the AF of  $t$ -Te, the present predictions may only be compared with those of  $t$ -Se.

The approximate coincidence of the zeros of  $B_v(\vec{r})$  with atomic separations, in addition to those resulting from the translation symmetry, which was first discovered for  $t$ -Se,<sup>4</sup> persists for  $t$ -Te with lesser precision. Since the positions of the additional zeros do not change essentially with  $\alpha$  the positions of these zeros must also be determined by structural and occupational effects.<sup>20</sup> A similar finding from a model based on the Weaire-Thorp Hamiltonian has recently been made for the tetrahedral phases of C, Si, and Ge.<sup>23</sup> The amplitudes of  $B_v(\vec{r})$  change more sensitively with  $\alpha$ . For correlation lengths  $l$  beyond the

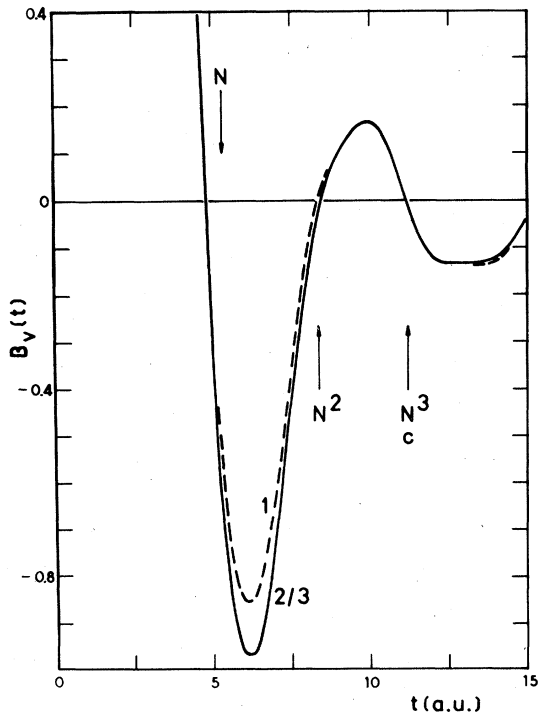


FIG. 5. Valence-electron autocorrelation function of one-electron density matrix  $B_v(\vec{r})$  for  $t$ -Te with  $\alpha = \frac{2}{3}$  and 1 as a function of  $t$  along the  $c$  axis. Atom separations along the chain from a common reference site are denoted with  $N^i$ , where  $i = 1$  is the nearest neighbor, etc. The norm is defined by  $B_v(0) = 18$ .  $t$  is in a.u.

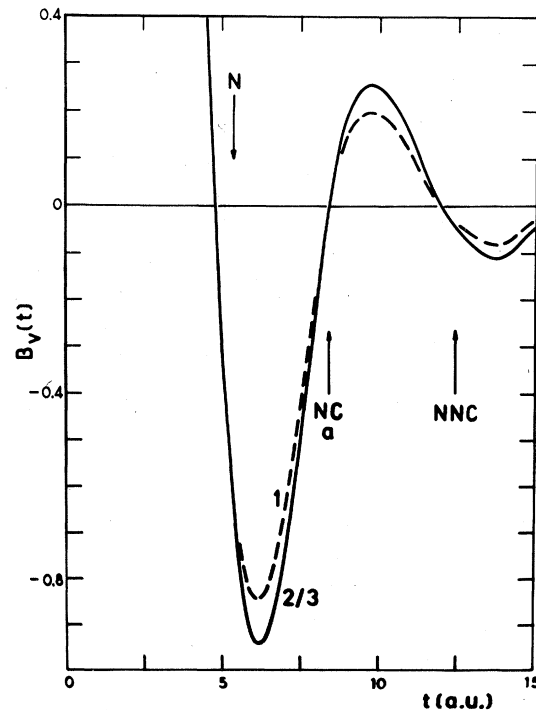


FIG. 6. Valence-electron autocorrelation function of one-electron density matrix  $B_v(\vec{r})$  for  $t$ -Te with  $\alpha = \frac{2}{3}$  and 1 as a function of  $t$  along the  $a$  axis. Atom separations are denoted with N, NC, and NNC. NC is the next chain site on the  $a$  axis and NNC the next site to NC. Units and norm are as in Fig. 5.

nearest-neighbor separation the present model with  $\alpha = \frac{2}{3}$  shows, especially for directions perpendicular to the  $c$  axis, larger oscillations than that with  $\alpha = 1$ . The interchain correlations for  $\alpha = \frac{2}{3}$  are of the order of 20% larger than  $\alpha = 1$ . Or, since the amplitude of  $B_v(\vec{r})$  beyond the nearest-neighbor separation also in an indirect manner measures the atom-atom interactions,<sup>4,21</sup> the interchain interactions in  $t$ -Te may be said to be considerably larger for the former value of  $\alpha$ . Intrachain correlations, on the other hand, are not appreciably affected by  $\alpha$  beyond the nearest-neighbor separations.

The comparison of the VAF of  $t$ -Te with that of  $t$ -Se (Refs. 4 and 8) results in important findings on the correlation differences in these two materials as measured by the autocorrelation function. The quantitative interpretation of these findings in terms of the more conventional quantities used to describe bonding and energetics is complicated by the fact that the AF represents a full ground-state property involving all states of the system. A set of simple models is therefore needed to facilitate interpretations. Since the construction of these models has not yet been fully completed,<sup>20</sup> any quantitative assignments in the following are of tentative nature only.

The amplitudes of  $B_v(\vec{r})$  at the first minimum differ by about 25% being larger for  $t$ -Te than  $t$ -Se. Since the amplitude at the first minimum for  $sp^n$ -bonded systems is most strongly influenced by the corresponding atomic AF and the nearest-neighbor interactions,<sup>21</sup> these interactions seem to be considerably larger in  $t$ -Te than in  $t$ -Se. Longer range intrachain correlations are in the average weaker in  $t$ -Te than in  $t$ -Se. The essential difference is seen in the directions perpendicular to the  $c$  axis at about the interchain separation and beyond it. Although the lattice constant values of  $t$ -Te and  $t$ -Se for  $a$  differ only by 2%, the amplitude of  $B_v(\vec{r})$  on the  $a$  axis at the first local maximum is for the latter by a factor of 3 larger. The next minimum of  $t$ -Se is already almost below resolution, whereas  $t$ -Te displays regularly decaying oscillations. Structural effects explain only a smaller part of this difference<sup>20</sup> and thus the interchain interactions in  $t$ -Te appear to be of the order of 3 times as strong as in  $t$ -Se. However, the decay of the amplitudes of  $B_v(\vec{r})$  along the  $a$  axis for  $t \geq a$  is still somewhat stronger than along the  $c$  axis, an expression of the trigonal anisotropy retained in  $t$ -Te. A comparison of the  $t$ -Te and  $t$ -Se VAF's with those derived from the isotropic FE model with the corresponding density shows, that for the former a qualitative agreement is obtained up to about  $t = 12$  a.u. and for the latter only up to about one-half of it.<sup>8</sup> Despite this fact, the decay properties of the VAF along the  $a$  axis for  $t > a$  also demonstrate that the  $t$ -Te ground state is still far from a transition into a monoclinic or cubic phase, which are to be expected at pressures of 45 (Ref. 24) and 60 kbar,<sup>25</sup> respectively.

## VI. CONCLUSIONS

The results in this paper for the charge density, momentum density, Compton profile, and autocorrelation function of the one-electron density matrix have all been obtained from a fully first-principles self-consistent approach with no adjustable parameters. The valence-electron charge density and its decomposition into triplet contributions has been shown to agree well with earlier pseudopotential results, although the present first-principles self-consistent charge densities have more fine structure. Apparently both full self-consistency and orthogonalization to the cores is needed to resolve the charge-density profiles in detail.

The present results for the momentum density, Compton profile, and autocorrelation function, are the first ones for  $t$ -Te. These quantities contain complementary information on the ground state, since they also depend on the off-diagonal parts of the one-electron density matrix. Especially the autocorrelation function reacts orders of magnitude stronger to changes in the chemical bonding than the charge density. Since no measurements for the Compton profile of  $t$ -Te exist, the predictions in this paper have to be verified later. A similar analysis has been performed for  $t$ -Se using the same methods. The excellent agreement of the  $t$ -Se results with  $\gamma$ -ray experiments supports the present predictions.

Important quantitative differences in the chemical bonding in  $t$ -Te and  $t$ -Se are found, if these are measured both in position space, by the charge density and the autocorrelation function, and in momentum space, by the momentum density and the Compton profile. The anisotropy of the charge and momentum density is substantially smaller in  $t$ -Te than in  $t$ -Se. The nearest-neighbor interactions in  $t$ -Te are larger than in  $t$ -Se, whereas further intrachain interactions appear to be slightly weaker in  $t$ -Te. The interchain interactions of  $t$ -Te exceed those of  $t$ -Se by a wide margin.

The quantitative information on the chemical bonding in  $t$ -Te is in agreement with conclusions deduced from infrared spectra<sup>26</sup> and Mössbauer spectra.<sup>25</sup> Additional Compton profile studies of the mixed crystal system  $\text{Se}_x\text{Te}_{1-x}$  would elucidate the increasingly molecular type of bonding, when proceeding from  $t$ -Te towards  $t$ -Se, even more.

## ACKNOWLEDGMENTS

Most of this work was carried out by all authors at the Electron Physics Laboratory of the Helsinki University of Technology. One of us (P.K.) wants to acknowledge the receipt of an ASLA-Fulbright research grant and to thank Professor Jeffrey Frey

for his kind hospitality during the completion of the present work at the Cornell University. Two of us (H. I. and J. v. B.) wish to express their gratitude to Professor M. A. Ranta for his continuous support. P. K. also gratefully acknowledges a travel grant for a visit to NORDITA from the Wihuri Foundation (Helsinki, Finland). The calculations were performed

on the Univac 1108 and 1100 computers at the Helsinki University of Technology and at NORDITA, respectively. Our sincere thanks go to the staffs of both computing centers for numerous services. We also wish to thank the Swedish Academy of Technical Sciences in Finland for financial support in connection with the publication.

\*At Cornell Univ., School of Electrical Engineering, Ithaca, N.Y. 14853.

†Present address: Helsinki Univ. of Technology, SF-02150 Espoo 15, Finland.

<sup>1</sup>For a recent review of the field see *Compton Scattering*, edited by B. G. Williams (McGraw-Hill, New York, 1977).

<sup>2</sup>P. Krusius, J. von Boehm, and T. Stubb, *Phys. Status Solidi* (b) **67**, 551 (1975).

<sup>3</sup>P. Krusius, *J. Phys. C* **10**, 1875 (1977).

<sup>4</sup>B. Kramer, P. Krusius, W. Schröder, and W. Schülke, *Phys. Rev. Lett.* **38**, 1227 (1977).

<sup>5</sup>G. G. Wepfer, R. N. Euwema, G. T. Surrat, and D. L. Wilhite, *Phys. Rev. B* **9**, 2670 (1974).

<sup>6</sup>A. Zunger and A. J. Freeman, *Phys. Rev. B* **15**, 5049 (1977); A. Zunger and A. J. Freeman, *Phys. Lett. A* **57**, 457 (1976).

<sup>7</sup>B. Kramer, P. Krusius, W. Schröder, and W. Schülke, in *Proceedings of the Seventh International Conference on Amorphous and Liquid Semiconductors*, edited by W. E. Spear (University of Edinburgh, Edinburgh, 1977).

<sup>8</sup>P. Krusius, in *The Physics of Selenium and Tellurium*, edited by E. Gerlach and P. Grosse (Springer, Berlin, 1979), Vol. 13, p. 12.

<sup>9</sup>H. Isomäki, J. von Boehm, P. Krusius, and T. Stubb, *Phys. Rev. B* **22**, 2945 (1980) (preceding paper).

<sup>10</sup>J. von Boehm, H. Isomäki, P. Krusius, and T. Stubb, in *The Physics of Selenium and Tellurium*, edited by E. Gerlach and P. Grosse (Springer, Berlin, 1979), Vol. 13, p. 20.

<sup>11</sup>In Ref. 3 the relative difference defined in the caption of Table I is given in percent.

<sup>12</sup>Additional data on the SCOPW ground-state models for  $t$ -

Te are available from the first author on request.

<sup>13</sup>E. Mooser, I. Ch. Schlüter, and M. Schlüter, *J. Phys. Chem. Solids* **35**, 1269 (1974); M. Schlüter, *Int. J. Quantum Chem.* **7**, 527 (1973).

<sup>14</sup>J. D. Joannopoulos, M. Schlüter, and M. L. Cohen, *Phys. Rev. B* **11**, 2186 (1975).

<sup>15</sup>Th. Starkloff and J. D. Joannopoulos, *Phys. Rev. B* **19**, 1077 (1979).

<sup>16</sup>D. J. Miller, D. Haneman, E. J. Baerends, and P. Ros, *Phys. Rev. Lett.* **41**, 197 (1978).

<sup>17</sup>The trigonal to cubic phase transition is discussed in detail for the valence-band triplets and the total charge density in Ref. 13.

<sup>18</sup>U. Bonse, W. Schröder, and W. Schülke, *Solid State Commun.* **21**, 807 (1977).

<sup>19</sup>P. Pattison, J. R. Schneider, and W. Schülke (unpublished); see also Ref. 8.

<sup>20</sup>P. Krusius and B. Kramer (unpublished).

<sup>21</sup>P. Krusius, H. Isomäki, and B. Kramer, *Phys. Rev. B* **19**, 1818 (1979).

<sup>22</sup>B. Kramer and P. Krusius, *Phys. Rev. B* **16**, 5341 (1977).

<sup>23</sup>A. MacKinnon and B. Kramer, *Solid State Commun.* **29**, 71 (1979).

<sup>24</sup>See, e.g., J. D. Joannopoulos, in *Physics of Selenium and Tellurium*, edited by E. Gerlach and P. Grosse (Springer, Berlin, 1979), Vol. 13, p. 2, and references therein.

<sup>25</sup>C. S. Kim and P. Boolchand, *Phys. Rev. B* **19**, 3187 (1979).

<sup>26</sup>R. M. Martin, G. Lucovsky, and K. Helliwelli, *Phys. Rev. B* **13**, 1383 (1976).